Guoxian Xiao
Graduate Research Assistant.

Stephen Malkin
Professor.
Fellow ASME

Kourosh Danai
Associate Professor.
Mem. ASME

Department of Mechanical Engineering,
University of Massachusetts,
Amherst, MA 01003

Autonomous System for Multistage Cylindrical Grinding

An optimization strategy is presented for cylindrical plunge grinding operations. The optimization strategy is designed to minimize cycle time while satisfying production constraints. Monotonicity analysis together with local linearization are used to simplify the non-linear optimization problem and determine the process variables for the optimal cycle. At the end of each cycle, the uncertain parameters of the process are estimated from sensory data so as to provide a more accurate estimation of the optimal process variables for the subsequent cycle. The optimization strategy is validated both in simulation and for actual grinding tests.

1 Introduction

Grinding is commonly utilized as a final machining operation in the production of precision components requiring smooth surfaces and fine tolerances. Although grinding operations are usually the most costly of all manufacturing processes, relatively little effort has been directed in industry toward their optimization. Optimization analyses for grinding, analogous to those for other types of machining operations, have been developed which are designed to minimize either cycle time or cost (Saljé et al., 1980; Peters and Aerens, 1980; Peters, 1984). However, the prospects for their implementation are limited because indicated "optimal" conditions often violate production constraints (Malkin, 1989). Furthermore, these analyses cannot cope with modeling uncertainty and process variability.

Optimal operating conditions for grinding are usually bounded by production constraints related either to the machine capability or the workpiece quality (Peters, 1984; Malkin, 1989). In recognition of the critical role of constraints, a practical constraint-limited optimization strategy was developed (Malkin, 1987) which utilizes an iterative process of increasing the removal rate (decreasing cycle time) until a constraint (bottleneck) is encountered, relaxing that constraint (if possible), and thereafter continuing to increase the removal rate until another constraint is encountered. This cycle time reduction strategy continually drives the cycle faster until either of the constraints (e.g., "burning power" or surface roughness) becomes tight, and then relaxes the tight constraint by changing the dressing parameters. This process is repeated until both of the constraints simultaneously become tight. While effective in coping with modelling uncertainty and process variability, this type of strategy is applicable only to those cases with two constraints which can each be relaxed by changing the dressing conditions in the opposite way. Moreover, the implementation of this iterative approach is generally slow and tedious, and therefore not suitable for computer control.

Contributed by the Dynamic Systems and Control Division for publication in the JOURNAL OF DYNAMIC SYSTEMS, MEASUREMENT, AND CONTROL. Manuscript received by the DSCD March 17, 1992; revised manuscript received February 9, 1993. Associate Technical Editor: A. G. Ulsoy.

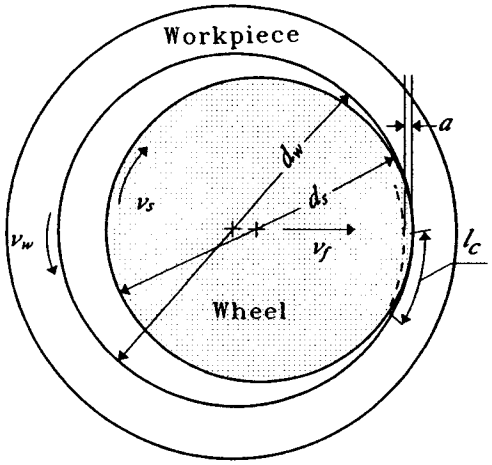

Fig. 1 Illustration of internal cylindrical plunge grinding

In the present paper, a new optimization strategy is presented for minimizing grinding cycle time while satisfying production constraints. The strategy utilizes parameter estimation to cope with modeling uncertainty and process variability by continually updating the estimated optimal conditions using parameters estimated from the preceding grinding cycle. Efficient estimation of the optimal point is based upon a simplified model of the process using a monotonicity analysis (Papalambros and Wilde, 1988) and local linearization. This optimization strategy provides the practical basis for control of the grinding cycle whereby the system is smart enough to achieve its optimal operating point in response to sensory data.

2 Grinding Cycle Basics

This section presents some background information about cylindrical plunge grinding cycles as a basis for developing the optimization strategy. Material removal in cylindrical grinding occurs by radially infeeding the wheel into the workpiece with a programmed infeed velocity of the cross-slide. This is illustrated in Fig. 1 for internal cylindrical grinding and would also

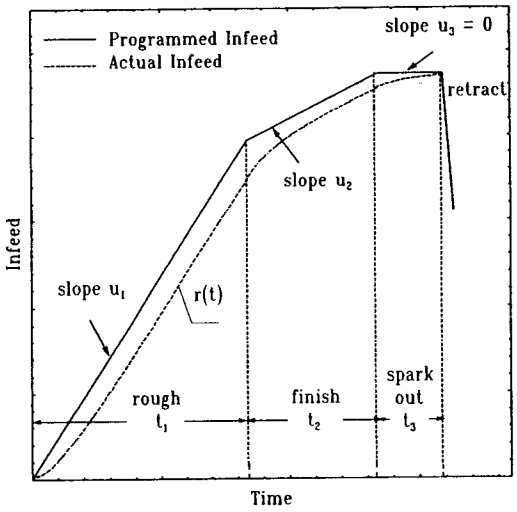

Fig. 2 Illustration of a grinding cycle consisting of roughing, finishing and spark-out stages

apply to external cylindrical grinding. The grinding infeed cycle (see Fig. 2) is typically divided into three stages each characterized by a discrete programmed infeed velocity $u(t)$: (1) roughing with a fast infeed velocity u_1, (2) finishing with a slower infeed velocity u_2, and (3) spark-out at zero infeed velocity ($u_3 = 0$). This is followed by rapid retraction to disengage the wheel from the workpiece. Specification of the grinding cycle requires not only values for u_1 and u_2, but also the time durations for each of the three sequential stages (t_1, t_2, and t_3), the peripheral workspeed v_w, and the dressing parameters (radial dressing depth a_d and dressing lead s_d).

In response to the programmed infeed $p(t)$ in Fig. 2, the actual radial size reduction of the workpiece follows the curve $r(t)$ with a slope corresponding to the actual infeed velocity $v_f(t)$ shown in Fig. 1. The transient in $r(t)$ at the beginning of each stage is attributed mainly to the elastic deflection of the system, and also to radial wear of the grinding wheel. This transient behavior can be approximated by a first-order system characterized by a time constant τ (Malkin, 1987).

In addition to specifying the parameters for controlling the infeed, it is also necessary to specify the dressing parameters associated with periodically shaping and conditioning the wheel. For example, with fixed point diamond dressing on conventional abrasive wheels, the parameters to be specified are the radial dressing depth a_d, the dressing lead s_d, and also the frequency of dressing (i.e., workpieces per dress). Finer dressing (smaller dressing lead and/or depth) results in a duller wheel, thereby causing higher grinding power, higher temperatures, and a greater tendency for thermal damage to the workpiece, but the resulting surface finish is smoother due to more even protrusion of the abrasive cutting points from the wheel surface (smoother wheel). This implies the existence of an optimal dressing condition which balances the need to satisfy a maximum surface roughness requirement against the need for maintaining the power below a critical value so as to avoid thermal damage to the workpiece (Malkin, 1989).

Machine control begins with gap elimination at the maximum infeed rate available. Other than machine limitations (e.g., available spindle power and part chucking capability), the infeed rate u_1 for the subsequent roughing stage is constrained by workpiece quality requirements including thermal damage and maximum surface roughness. Two thermal damage constraint scenarios are considered: (1) no thermal damage at all during the cycle (no-burn constraint) in which case it is necessary to keep the grinding zone temperature below a critical value throughout the cycle, and (2) thermal damage restricted to a certain depth during the roughing stage which is completely removed during the subsequent finishing stage (burning constraint). The grinding power can be expected to reach but not exceed the corresponding allowable burning power limit at the end of the roughing stage for the no-burn constraint, and exceed the burning power limit when the burning constraint is active. The burning constraint is less restrictive than the no-burn constraint and should therefore lead to a shorter optimal cycle.

The roughing stage is followed by an intermediate finishing stage (see Fig. 2) which may be required to (1) remove a thermally damaged layer from the previous roughing stage [2], (2) control size, (3) improve surface finish, and (4) control roundness. If the burning constraint applies, burning from the roughing stage will persist into the finishing stage until the actual infeed rate is sufficiently reduced during the transient. From the finishing stage the process proceeds to spark-out with zero programmed infeed rate, during which the workpiece is rounded up and the surface finish improved at a diminishing rate as the elastic deflection of the machine is recovered. The cycle is terminated and the wheel rapidly retracted when the final size is reached as indicated by the size gage measurement. It should be noted that the final size can be reached only if the deflection at the end of the prior finishing stage exceeds the radial allowance to be removed during spark-out.

An autonomous grinding system should be able to adjust its own operating parameters to minimize cycle time subject to production and workpiece quality constraints in response to measurements from sensors. As a practical matter, the only in-process sensors which can be reliably utilized in a harsh production environment are a power monitor which measures the wheel spindle power, and a size gage which measures the workpiece diameter (Rao and Malkin, 1990). The power monitor output can be used to identify initial wheel-workpiece

Nomenclature

a = depth of cut
a_d = dressing depth
A_0 = constant
A_{eff} = effective dullness
d_e = equivalent diameter
d_w = diameter of part
d_s = diameter of wheel
f = modified coefficient
G = grinding ratio
k = thermal conductivity of part
l_c = contact length
m = constant
n_w = rotational speed of workpiece
P = grinding power
P_b = burning power
q_i = actual infeed for the ith stage
r = actual value of out-of-roundness
r_0 = constant
R_a = measured surface finish
R_0 = constant
s_d = dressing lead
t_i = grinding time for the ith stage
u = specific energy
u_{ch} = specific energy for chip formation
u_i = programmed infeed rate
u_i = effective programmed infeed rate
v_f = actual infeed rate
v_i = actual infeed rate for the ith stage
v_s = velocity of wheel
v_w = velocity of workpiece
x = constant
y = constant
z = depth of burn
α = thermal diffusivity of part
β = fraction of finishing stage with burning
δ = equivalent dressing infeed angle
γ = constant
θ_{mb} = critical temperature for burning
τ = time constant

Table 1 Grinding conditions used for nonlinear programming examples

Grinding conditions	Case 1	Case 2	Case 3
Wheel spec.	32A80L6	32A80M6	32A80O7
Wheel dia. (mm)	50	50	25
Wheel speed (m/s)	37	45	30
Work material	AISI 52100	AISI 52100	AISI 52100
Work diameter (mm)	70	100	50
Hardness (R_c)	60	60	60
Grinding width (mm)	9	9	9
Δx (mm)	0.25	0.25	0.25
u_l (mm/s)	0.002	0.002	0.002
u_u (mm/s)	0.035	0.025	0.045
R_{max} (μm)	0.7	0.7	0.7
r_{max} (μm)	0.6	0.6	0.6
τ (s)	1.4	1.4	1.7

engagement for gap elimination, to estimate the effective wheel dullness A_{eff}, and to indicate whether thermal damage is occurring and, if so, to estimate the depth of the damaged layer z_1 on the workpiece. The output from the size gage, which directly indicates the remaining radial allowance to be removed, can also be used to estimate the elastic deflection of the system and the radial wheel wear (or grinding ratio G). The information derived from these two in-process sensors, together with post-process measurement (inspection) of part quality (e.g., finish and roundness), will be used to estimate the optimal process variables for control of the cycle.

3 Optimization Analysis

Based on the description of the process presented above, specification of the grinding operation requires selection of ten independent variables: two infeed velocities u_1 and u_2, time durations for the three stages t_1, t_2, and t_3, dressing depth a_d, dressing lead s_d, dressing frequency, wheel velocity v_s, and work velocity v_w. The optimization problem can be greatly simplified if the number of the independent variables is reduced. In practice, the dressing depth a_d is usually held constant and the dressing lead s_d varied to alter the dressing severity. Furthermore, it can be shown that automation of the dressing operation so that the associated non-productive time becomes an insignificant portion of the total cycle would indicate an optimal dressing frequency of once per part (Malkin, 1987). The peripheral velocity v_s is usually limited by safety considerations, so it too is held constant. Simulation results indicate that the peripheral work velocity v_w has a secondary influence on the cycle time, so it is not included as an independent variable in this problem.

In view of the above considerations, the number of independent variables can be reduced to six. The optimization problem can now be defined mathematically as:

$$\text{Minimize cycle time: } \Phi = t_1 + t_2 + t_3$$
$$\text{with respect to: } u_1, u_2, t_1, t_2, t_3, s_d \quad (1)$$

subject to the constraints:

$$g_1 = P_m(u_1, A_{eff}) - P_b(u_1) \le 0 \text{ (no-burn constraint)} \quad (2)$$
$$g_2 = z_1(u_1, A_{eff}) - q_2(u_1, u_2, t_2, \tau) \le 0 \text{ (burning constraint)} \quad (3)$$
$$g_3 = R_a(u_1, s_d) - R_{max} \le 0 \text{ (surface finish constraint)} \quad (4)$$
$$g_4 = r(u_1, u_2, t_2, t_3, \tau) - r_{max} \le 0 \text{ (out-of-roundness constraint)} \quad (5)$$
$$g_5 = u_1 t_1 + u_2 t_2 - \Delta r = 0 \text{ (size constraint)} \quad (6)$$
$$g_6 = u_l - u_i \le 0 \quad i = 1,2 \text{ (lower infeed constraint)} \quad (7)$$
$$g_7 = u_i - u_u \le 0 \quad i = 1,2 \text{ (upper infeed constraint)} \quad (8)$$

In the above model, the inequality g_1 defines the power for the no-burn constraint, where P_m is the maximum power during the cycle, P_b represents the burning power limit, and A_{eff} denotes the effective wheel dullness which depends on the wheel, workpiece material, and dressing conditions. The inequality g_2 defines the depth of workpiece burn for the burning constraint, where z_1 represents the depth of workpiece burn produced during the roughing stage and q_2 the depth of removal in the subsequent finishing stage. In the limit with $z_1 = 0$, this constraint reverts to the no-burn constraint. The inequality g_3 defines the surface finish requirement where R_a denotes the actual surface roughness and R_{max} its maximum allowable value. The inequality g_4 defines the out-of-roundness requirement where r is the actual value of out-of-roundness (mainly dependent on t_3 and τ), and r_{max} is its maximum allowable value. The equality g_5 defines the size requirement where Δr denotes the radial workpiece allowance. For formulating the mathematical problem, the size constraint in Eq. (6) indicates zero tolerance and neglects wheel wear. However, these effects are actually taken into account by direct size measurements at the end of the spark-out stage. The last two constraints (Eqs. (7) and (8)) represent limitations on the machine infeed rates—u_l represents the lower bound and u_u the upper bound. The detailed relationships among the process variables, process parameters, and part constraints are included in the Appendix.

Table 2 Coordinates of the optimal point obtained from nonlinear programming for the grinding conditions listed in Table 1 and optimal points

Optimal variables	Case 1	Case 2	Case 3
u_1^* (mm/s)	0.0268	0.018	0.036
u_2^* (mm/s)	0.002	0.002	0.002
t_1^* (s)	9.03	13.38	6.67
t_2^* (s)	3.88	4.54	4.88
t_3^* (s)	3.65	3.42	3.27
s_d^* (mm)	0.0657	0.082	0.13
Φ^* (s)	16.56	21.34	14.82
Constraint Values			
g_1 (kW)	NA	NA	NA
g_2 (mm)	−0.81E-4	−0.18E-3	−0.21E-3
g_3 (μm)	0.84E-3	−0.66E-3	0.56E-3
g_4 (μm)	−0.006	−0.010	−0.017
g_5 (mm)	0.0	0.0	0.0
g_6 (mm/s)	0.0	0.0	0.0

In order to study the characteristic of the optimal point, the optimization problem of Eq. (1) was solved using the nonlinear programming package OPTDES (Parkinson and Wilson, 1988). The optimal process variables obtained for the conditions listed in Table 1 are included in Table 2. The results in Table 2 indicate that the optimal infeed rate during the finishing stage is equal to its lower bound (i.e., $u_2^* = u_l$), and that all the constraints g_2, g_3, g_4, g_5, and g_6 are tight at the optimal point. The constraint g_2 prevails over g_1 because a shorter cycle time can be achieved with the burning constraint than with the no-burn constraint. This will be considered in more detail later in the paper.

4 Monotonicity Analysis

In the previous section, the optimal grinding conditions were obtained using nonlinear programming. However, in order to implement an autonomous grinding system, whereby the optimal operating variables are found in response to sensory data, a closed-form solution to the optimization problem is needed. For this purpose, the problem can be simplified through monotonicity analysis (Papalambros and Wilde, 1988) as follows:

- The objective function (see Eq. (1)) is a monotonically increasing function of t_2 and t_3 (i.e., $\Phi(t_2^+)$ and $\Phi(t_3^+)$), and g_2 and g_4 are the only monotonically decreasing functions of t_2 and t_3, respectively (i.e., $g_2(t_2^-)$ and $g_4(t_3^-)$). Therefore, according to the First Monotonicity Principle (MP1)[1] both of the constraints g_2 and g_4 are critical and

[1] In a well-constrained objective function every increasing (decreasing) variable is bounded below (above) by at least one active constraint (Papalambros and Wilde, 1988).

active. As such, they can be converted to equality constraints (i.e., $g_2 = 0$ and $g_4 = 0$), and t_2 and t_3 can be defined in terms of the other process variables to eliminate them from the objective function.

- The reduced model obtained by elimination of t_2 and t_3 indicates that the objective function is a monotonically decreasing function of s_d (i.e., $\Phi(s_d^-)$). Since g_3 is the only monotonically increasing function of s_d (i.e., the $g_3(s_d^+)$), according to the MP1 g_3 is also critical and active (i.e., $g_3 = 0$ at the optimal point).
- The monotonicity of the partial derivative of the objective function with respect to u_2 should be studied for the burning constraint, where the cycle time is expected to be minimum. In order to quantify the duration of burning during the cycle, a parameter $0 \le \beta < 1$ is defined

$$\beta = (t_c - t_1)/t_2 \tag{9}$$

which denotes the fraction of the finishing stage during which burning persists. (The equality $\beta = 0$ would apply to the no-burn constraint and $0 < \beta < 1$ to the *burning constraint.*) Introducing β into the objective function and taking its derivative with respect to u_2 yields

$$\frac{\partial \Phi}{\partial u_2} = \frac{t_1[\exp(\beta t_2/\tau) - 1] - t_2}{u_1} \tag{10}$$

which is positive for

$$\beta > \frac{\tau}{t_2} \ln\left(1 + \frac{t_2}{t_1}\right) \tag{11}$$

In this case the objective function is a regionally monotonically increasing function of u_2 (i.e., $\Phi(u_2^+)$), and since the constraint g_6 is a monotonically decreasing function of u_2 (i.e., $g_6(u_2^-)$), according to the MP1 it is critical and active in the region defined by Eq. (11). The condition of Eq. (11) is generally found to be satisfied at the optimal point. However, in cases where the validity of Eq. (11) is questionable, the parameter β can be included as a design variable and Eq. (11) as an additional constraint in the optimization problem.

Based upon the monotonicity analysis presented above, the constraints g_2, g_3, g_4, and g_6 are tight at the optimal point, so they can be written as equalities.

5 Cycle Time Optimization Strategy

The optimization problem defined in Eqs. (1)–(8) contains six variables: u_1, u_2, t_1, t_2, t_3, and s_d. One approach to solve for these optimal variables might be to combine the equality constraints g_2, g_3, g_4, and g_6 together with the equality g_5 to obtain the variables t_1^*, t_2^*, t_3^*, u_2^*, and s_d^*, which could then be eliminated from the objective function to obtain u_1^* (i.e., $u_1^* = \arg(\min \Phi)$). But due to the nonlinearity of these equations, this does not provide a closed-form solution. A partial solution, however, can be obtained by defining the variables u_2^*, t_1^*, and t_3^* in terms of the other three variables u_1^*, t_2^*, and s_d^* as:

$$u_2^* = u_l \quad (\text{from } g_6 = 0) \tag{12}$$

$$t_1^* = \frac{\Delta r - u_l t_2^*}{u_1^*} \quad (\text{from } g_5 = 0) \tag{13}$$

$$t_3^* = r_0 \tau \ln\left(\frac{u_l}{r_{\max}}\right) \quad (\text{from } g_4 = 0) \tag{14}$$

where r_0 in Eq. (14) denotes a constant. Since the three variables u_1^*, t_2^*, and s_d^* cannot be computed from the corresponding set of nonlinear equations $g_2 = 0$, $g_3 = 0$ and $d\Phi/du_1 = 0$ ($\mathbf{H} = 0$), they need to be estimated. For this purpose, the set of equations $\mathbf{H} = 0$ are expanded through Taylor series as

$$\mathbf{H}|_{\mathbf{X}=\mathbf{X}_{i+1}} = \mathbf{H}|_{\mathbf{X}=\mathbf{X}_i} + \left[\frac{\partial \mathbf{H}}{\partial \mathbf{X}}\bigg|_{\mathbf{X}=\mathbf{X}_i}\right]\Delta \mathbf{X} \tag{15}$$

where $\mathbf{X}$ denotes the vector of variables u_1, t_2, and s_d, $\Delta\mathbf{X}$ represents the incremental modification of the process variables, i represents the iteration step, and $\partial\mathbf{H}/\partial\mathbf{X}$ denotes the Jacobian matrix. Based on Eq. (15), the solution for $\Delta\mathbf{X}$ is obtained such that

$$\mathbf{H}|_{\mathbf{X}=\mathbf{X}_{i+1}} = 0$$

to provide the estimation algorithm for $\Delta\mathbf{X}$ as

$$\Delta \mathbf{X} = \left[\frac{\partial \mathbf{H}}{\partial \mathbf{X}}\bigg|_{\mathbf{X}=\mathbf{X}_i}\right]^{-1} [-\mathbf{H}|_{\mathbf{X}=\mathbf{X}_i}] \tag{16}$$

Note that accurate estimation of the optimal variables u_1^*, u_2^*, t_1^*, t_2^*, t_3^*, and s_d^* depends upon the validity of the mathematical model of the process (e.g., see the Appendix). As such, any modeling inaccuracy could cause the algorithm to overshoot the target $\mathbf{H} = 0$ and damage the workpiece. To avoid this situation, (1) the uncertain parameters of the model are estimated and updated at the end of each cycle, and (2) a margin of modeling error ϵ associated with $\mathbf{H}$ is used which yields

$$\Delta \mathbf{X} = \left[\frac{\partial \mathbf{H}}{\partial \mathbf{X}}\bigg|_{\mathbf{X}=\mathbf{X}_i}\right]^{-1} (\epsilon - \mathbf{H}|_{\mathbf{X}=\mathbf{X}_i}) \tag{17}$$

The margin of modeling error ϵ denotes the inaccuracy of the model in representing

$$\mathbf{H} = \begin{pmatrix} z_1 - q_2 \\ R_a - R_{\max} \\ d\Phi/du_1 \end{pmatrix}$$

and can be specified based on our confidence in the model to represent the parameters z_1 and R_a. Note that the margin of modeling error associated with $d\Phi/du_1$ is zero.

The estimation algorithm presented above requires values for some parameters, namely, the time constant of the equivalent first order system τ, the grinding ratio G, and the effective wheel dullness A_{eff}, which are not known a priori. The time constant τ is estimated based on the infeed transient at the beginning of the roughing stage using least square parameter estimation techniques (Ljung, 1987). The grinding ratio G, which is the volumetric ratio of material removal to wheel wear, is estimated from the difference between the controlled infeed velocity $u(t)$ and the slope of the actual size reduction curve $r(t)$ (see Fig. 2). Linear regression is used to estimate the slope of actual infeed rate after the initial transient in the roughing stage. The effective wheel dullness A_{eff} is estimated at the end of each cycle by matching the measured power against its computed values throughout the cycle (see Eq. (26) in the Appendix) using the least square criterion.

Based on the above analysis, a cycle time optimization strategy is formulated as follows: The first cycle is run conservatively with the process variables u_1^0, u_2^0, t_1^0, t_2^0, t_3^0, s_d^0 so as to estimate the parameters τ, G, and A_{eff}. After the first cycle, the optimal process variables for an intermediate cycle with the no-burn constraint ($\beta = 0$) is found. The process variables u_1^1 and s_d^1 for this intermediate cycle are estimated using the constraint $g_1 = 0$ in place of $g_2 = 0$ in Eq. (17) with $g_3 = 0$. The parameter t_2^1 is set equal to the approximate transient time 3τ, and the other variables u_2^1, t_1^1, and t_3^1 are obtained using Eqs. (12)–(14). At the end of the second cycle, the estimation algorithm defined by Eq. (17) along with Eqs. (12)–(14) can then be used to estimate the optimal process variables for the third cycle with the burning constraint ($0 < \beta < 1$). This is achieved by estimating the incremental modification $\Delta\mathbf{X}$ for each of the process variables u_1^1, u_2^1, t_1^1, t_2^1, t_3^1, s_d^1 from Eq. (17) to yield the optimal variables u_1^*, u_2^*, t_1^*, t_2^*, t_3^*, and s_d^*.

Table 3 Estimated parameters, process variables dictated by the cycle-time optimization strategy, and the values of the constraints for the three simulated cycles

Estimated parameters	Cycle 1	Cycle 2	Cycle 3
$\hat{\tau}$ (s)	1.58	1.4	1.34
$\hat{G}$	21.5	15.8	7.2
$\hat{A}_{\text{eff}}$	0.008	0.015	0.022
Grinding variables			
u_1 (mm/s)	0.012	0.017	0.0254
u_2 (mm)	0.004	0.002	0.002
t_1 (s)	16.8	14.2	9.5
t_2 (s)	10	4.7	3.8
t_3 (s)	5	4.4	3.7
s_d (mm)	0.137	0.104	0.066
Constraint values			
g_1 (kW)	−0.41	0	NA
g_2 (mm)	NA	−0.012	0
g_3 (μm)	−0.06	0	0
g_4 (μm)	−0.14	0	0
g_5 (mm)	0	0	0
g_6 (mm/s)	−0.002	0	0
Cycle time (s)	31.8	23.3	17.0

6 Verification in Simulation

Prior to implementation on an actual system, the proposed cycle time optimization strategy was investigated in simulation using the grinding simulation software ALFRED (Chiu, 1989) developed at the University of Massachusetts. This simulation is based upon the same models in the Appendix as for the optimization strategy. The grinding conditions used for simulation were those for Case 1 of Table 1. For these conditions, the estimated process parameters, the values of process variables, and the values of constraints at the end of each cycle are listed in Table 3. The results indicate that the proposed cycle time optimization strategy reduces the cycle time from 31.8 seconds in Cycle 1 down to 23.3 seconds in Cycle 2 (no-burn constraint) and 17.0 seconds in Cycle 3 (burning constraint). The simulation results for the infeed, depth of burn, and power during Cycle 3 with the burning constraint are shown in Fig. 3. During most of the roughing stage and part of the finishing stage up to time t_c, the grinding power exceeds the corresponding burning power P_b.

The optimal variables obtained from the proposed cycle-time optimization strategy with the burning constraint must satisfy the condition that thermal damage from the roughing stage is completely removed in the finishing stage. This condition is satisfied if:

$$u_1 + \left.\frac{\partial z}{\partial t}\right|_{t=t_1} \leq 0 \tag{18}$$

Simulation results generally show that this condition is automatically satisfied by the algorithm of Eq. (17). However, if this condition is not satisfied, Eq. (18) can then be used as an equality constraint to determine u_1^*.

7 Experimental Implementation

The proposed cycle-time optimization strategy was experimentally implemented on the grinding system illustrated in Fig. 4. This system consists of a Bryant Model 1116 internal grinder modified by the addition of a stepper motor infeed drive, an electrical workpiece drive in place of the original hydraulic motor for computer control, a power monitor (A.F. Green TT2), and a diametral size gage (Marposs Micromar 5 and E9 amplifier) with a personal computer for data acquisition and control (Rao and Malkin, 1990). The grinding conditions used in the experiments were the same as those used in the simulation (Case 1 of Table 1). No instrument was available to measure out-of-roundness, so this is not given in Table 1.

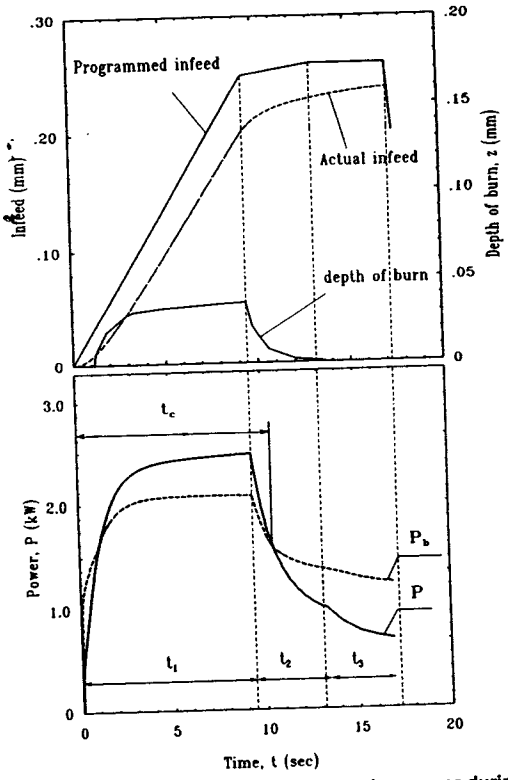

Fig. 3 Infeed, depth of burn, power and burning power during the optimal cycle of Case 1 in Table 1

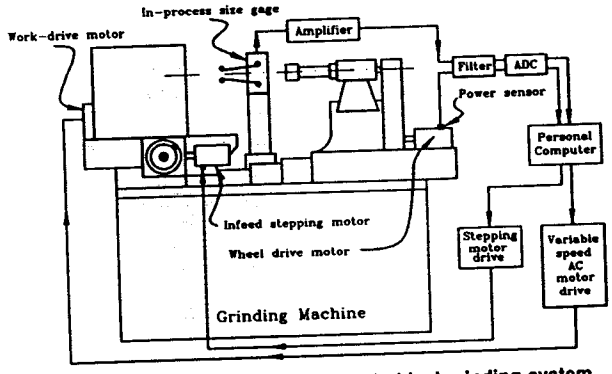

Fig. 4 Illustration of the internal cylindrical grinding system

The estimated parameters, the process variables from the optimization strategy, and values of the constraints at the end of each cycle are included in Table 4, and the programmed and actual infeeds for the three cycles in Table 4 are shown in Fig. 5. These results are remarkably close to those obtained for the simulation, which reflects the validity of the grinding model. The nonlinear nature of the process model is apparent from the variation of the values for $\hat{\tau}$, $\hat{G}$, and $\hat{A}_{\text{eff}}$ estimated at the end of each cycle. The cycle time optimization strategy reduced the cycle time from 31.8 seconds in Cycle 1 down to 22.7 seconds in Cycle 2 (no-burn constraint), and 16.6 seconds in Cycle 3 (burning constraint). For Cycle 1, the constraints g_1 and g_3 are much smaller than zero indicating that the grinding power is less than the burning power at the end of the roughing stage ($P_m/P_b = 0.87$) and the surface roughness ($R_a = 0.63$ μm) is less than its maximum allowed value ($R_{\max} = 0.70$ μm). For Cycle 2, the roughing infeed u_1 is raised so that $g_1 = 0$ and the dressing condition is adjusted so that $g_3 = 0$. It should be noted that the actual grinding power and surface roughness values obtained in Cycle 2 were almost identical to their intended constrained values ($P_m/P_b = 0.99$ and $R_a = 0.70$ μm).

Table 4 Estimated parameters, process variables, and constraint values experimentally obtained for the three consecutive cycles

Estimated parameters	Cycle 1	Cycle 2	Cycle 3
$\hat{\tau}$ (s)	1.60	1.32	1.31
$\hat{G}$	22.6	14.7	8.2
$\hat{A}_{\text{eff}}$	0.01	0.0162	0.021
Grinding variables			
u_1 (mm/s)	0.012	0.018	0.027
u_2 (mm/s)	0.004	0.002	0.002
t_1 (s)	16.8	13.5	9.0
t_2 (s)	10.0	4.8	3.9
t_3 (s)	5.0	4.4	3.7
s_d (mm)	0.137	0.102	0.064
Constraint values			
g_1 (kW)	−0.48	0	NA
g_2 (mm)	NA	NA	NA
g_3 (μm)	−0.07	0	−0.01
g_4 (μm)	−0.12	0	0
g_5 (mm)	0	0	0
g_6 (mm/s)	−0.002	0	0
Others			
R_a (μm)	0.63	0.70	0.69
P_m/P_b	0.87	0.99	1.22
Cycle time (s)	31.8	22.7	16.6

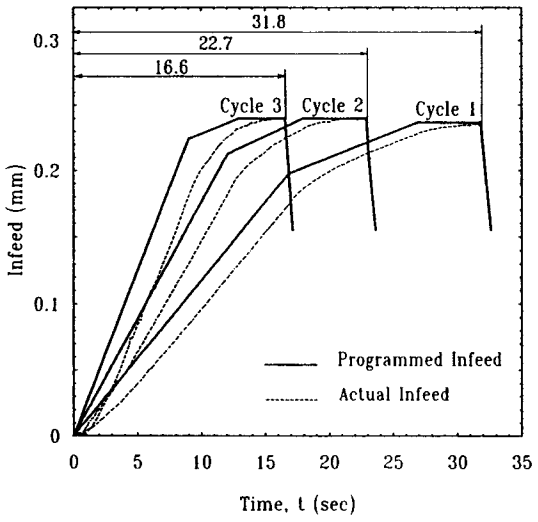

Fig. 5 Programmed and actual infeeds for the three successive cycles using the cycle-time optimization strategy

In Cycle 3, the constraint g_2 is activated to further reduce the cycle time. In this case, the grinding power at the end of the roughing stage exceeds the corresponding estimated burning power (P_m/P_b = 1.22) as expected, and the final roughness (R_a = 0.60 μm) is again very close to its maximum allowed value. Although not included in Table 4, the cycle-time optimization strategy also gave virtually identical optimal results for Cycle 2 and Cycle 3 when using different initial grinding conditions for Cycle 1.

Acknowledgment

This work was supported by a grant from the National Science Foundation (grant No. DDM-9114484).

References

Chiu, N., 1989, "Computer Simulation for Cylindrical Plunge Grinding," Master's thesis, University of Massachusetts, Amherst.

Ljung, L., 1987, *System Identification: Theory for the User*, Prentice-Hall, Englewood Cliffs, NJ.

Malkin, S., 1989, "Grinding Technology: Theory and Application of Machining with Abrasives," Chapter 10, *Optimization, Adaptive Control, and Intelligent Grinding*, John Wiley & Sons, New York.

Malkin, S., 1987, "Practical Grinding Optimization," *Manufacturing Technology Review*, SME Paper No. MR 86-637, pp. 123-140.

Papalambros, P., and Wilde, D., 1988, *Principles of Optimal Design*, Cambridge Univ. Press, New York, NY.

Parkinson, A., and Wilson, M., 1988, OPTDES.BYU, Technical Report, Brigham Young University, Salt Lake City, Utah.

Peters, J., 1984, "Contribution of the CIRP Research to Industrial Problems in Grinding," *Annals of the CIRP*, Vol. 33, No. 2, pp. 451-468.

Peters, J., and Aerens, R., 1980, "Optimization Procedure of Three Phase Grinding Cycles of a Series Without Intermediate Dressing," *Annals of the CIRP*, Vol. 29, No. 1, pp. 195-199.

Rao, A., and Malkin, S., 1990, "Process Monitoring for Intelligent Control of Grinding," 4th International Grinding Conference, pp. 512-1-512-11.

Saljé, E., Mushardt, H., and Sherf, E., 1980, "Optimization of Short Grinding Cycles," *Annals of the CIRP*, Vol. 29, No. 2, pp. 477-495.

APPENDIX

The following equations obtained from grinding theory are used for calculating and estimating the process parameters (Malkin, 1989):

$$a = v_f/n_w \tag{19}$$

$$n_w = v_w/(\pi d_w) \tag{20}$$

$$d_e = (d_s d_w)/(d_w - d_s) \tag{21}$$

$$v_i = u_i' - (u_i' - v_{i-1})\exp\left(-\frac{t_i}{\tau}\right) \tag{22}$$

$$q_i = u_i' t_i + \tau\left[(u_i' - v_{i-1})\exp\left(-\frac{t_i}{\tau}\right) - (u_i' - v_{i-1})\right] \quad i = 1,2,3 \tag{23}$$

$$u_i' = u_i/f \tag{24}$$

$$f = 1 + d_w/(d_s G) \tag{25}$$

$$P = .0138\pi d_w v_f + 9.62\times 10^{-7} v_s + [8.55\times 10^{-6} + 2.10 v_w/(v_s d_e)] v_s v_w^{-.5} (\pi d_w v_f d_e)^{.5} A_{\text{eff}} \tag{26}$$

$$P_b = 0.00617\pi d_w v_f + 0.0072(\pi d_w d_e v_f v_w)^{0.25} \tag{27}$$

$$z = -1.449\left(\frac{v_w l_c}{4\alpha}\right)^{0.37} \frac{2\alpha}{v_w} \ln \times \left[\frac{\pi k l_c \theta_{mb} v_w}{6.2\alpha\pi d_w v_f \left(\frac{v_w l_c}{4\alpha}\right)^{0.53} (u - 0.45 u_{ch})}\right] \tag{28}$$

$$u = P/(\pi d_w v_f) \tag{29}$$

$$l_c = (\pi d_w d_e v_f/v_w)^{0.5} \tag{30}$$

$$r = \pi r_0 v_3 d_w/v_w \tag{31}$$

$$R_a = R_0 S_d^x a_d^y \left(\frac{\pi d_w v_1}{v_s}\right)^{\gamma} [1 + \exp(-0.1345 t_3)] \tag{32}$$

$$A_{\text{eff}} = -0.008 A_0 \ln(1.4\times 10^4 m\delta) \tag{33}$$

$$\delta = 1.1\times 10^{-11} a_d^{0.75} s_d^{1.75} \tag{34}$$

$$\tau = f(u_1 t_1 - f q_1)/u_1 \tag{35}$$

$$G = (\pi v_1 d_w)/(\pi w_1 d_s) = (v_1 d_w)/[(u_1 - v_1) d_s] \tag{36}$$